

Nanoparticles dispersion in processing functionalised PP/TiO₂ nanocomposites: distribution and properties

Hassan M. El-Dessouky · Carl A. Lawrence

Received: 10 March 2010 / Accepted: 21 September 2010 / Published online: 9 October 2010
© Springer Science+Business Media B.V. 2010

Abstract Future innovations in textiles and fibrous materials are likely to demand fibres with enhanced multifunctionality. The fibres can be functionalized by dispersing nanoadditives into the polymer during melt compounding/spinning. TiO₂ nanoparticles have the potential to improve UV resistance, antistatic, as well as impart self-cleaning by photocatalysis and thereby de-odour and antimicrobial effects. In this study, a micro-lab twin-screw extruder was used to produce samples of polypropylene (PP) nanocomposite monofilaments, doped with nano titanium oxide (TiO₂)/manganese oxide (MnO) compound having size ranging from 60 to 200 nm. As a control sample, PP filaments without additives were also extruded. Three samples were produced containing different concentrations (wt%) of the TiO₂ compound, i.e. 0.95, 1.24 and 1.79%. Nano metal-oxide distribution in the as-spun and drawn nanocomposite filaments was analysed. Although, there are small clusters of the nanoparticles, the characterizing techniques showed good dispersion and distribution of the

modified TiO₂ along and across the processed filaments. From UV spectroscopy and TGA, a significant enhancement of polypropylene UV protection and thermal stability were observed: PP with higher percentage of TiO₂ absorbed UV wavelength of 387 nm and thermally decomposed at 320.16 °C accompanied by 95% weight loss.

Keywords Nanotechnology · Nanoparticles · Titanium oxide · Polypropylene · Nanocomposites · UV · TGA · SEM · Fibers · Textiles

Introduction

In recent years, polymer-nanoparticle composites have attracted the interest of many researchers due to their great potential as multifunctional materials for a wide variety of applications. In textiles, nanoparticle additives such as TiO₂, ZnO, Ag, clay, CNT, etc. in synthetic fibres, can appreciably enhance fabric characteristics such as self-cleaning, softness for improved wearer comfort, high tensile strength, durability, water repellency, dyeability, colouration, conductivity, fire retardation, anti-microbial (bacterial), anti-static and UV-protection (Sawhney et al. 2008; Wong et al. 2006; Pane et al. 2001; Jose and Abdul 1999; Wang and Li 2002; Ash et al. 2002).

At the micro-scale, TiO₂ as a white pigment has been used as just a delustrant in synthetic fibres for

H. M. El-Dessouky (✉) · C. A. Lawrence
Fibres Research Lab, School of Design,
University of Leeds, Leeds LS2 9JT, UK
e-mail: hassanoptics@yahoo.com

C. A. Lawrence
e-mail: c.a.lawrence@leeds.ac.uk

H. M. El-Dessouky
Physics Department, Faculty of Science,
Mansoura University, Mansoura, Egypt

many years. However, the development of TiO₂ nanoparticles, because of their larger total surface area per unit volume, provides the opportunity to exploit this metal-oxide's unique optical, electrical and chemical attributes in synthetic fibres; nanosized TiO₂ should give enhanced UV protection by scattering UV rays through its high refractive index and/or by absorbing UV rays because of its semiconductive properties, an additional benefit being antimicrobial effect from photocatalysis. Although TiO₂ particles have already been used as a compound of coating material in finishing processes, only a few studies have been published on the characterization of fibres modified with TiO₂ nanoparticles (Schmidt and Malwitz 2003; Wei et al. 2007; El-Dessouky et al. 2009; Erdem et al. 2010; Yeo et al. 2003).

In the study reported here, melt-compounding of nanoparticles was used in producing PP–TiO₂ nanocomposite monofilaments. Polypropylene (PP) is a widely used thermoplastic polymer in textile applications, because of its low cost, easy processing, low density, high tensile strength, and good chemical stability. However, there are disadvantages, such as low polarity, poor ultraviolet (UV), non-bacterial resistance and low thermal stability. For example, in this study, the addition of TiO₂ nanoparticles is to improve UV protection and thermal stability of PP fibres based on previous studies, and inorganic nanoparticles enhance polymer stability (Kumar et al. 2009; Alexandre and Dubois 2000; Ray and Okamoto 2003; Chiu et al. 2010).

The uniform distribution of nanoparticles particles throughout bulk of PP fibres is an important factor, and will depend on the effectiveness of the mixing process before extrusion, that is to say, the extent to which the particles may aggregate during mixing and subsequent extrusion (Wei et al. 2007). This study is concerned with the uniformity of nanoparticle distribution obtained with a 10-mm twin-screw extruder in producing the nanocomposites as well as enhancing the physical properties of PP fibres.

Nano TiO₂ modified by MnO was compounded with PP, and four samples of monofilaments were melt-spun using a draw-down ration (DDR) and draw ratio (DR) of 11.18 and 13, respectively. A control, PP without any additive, and three doped with the following concentrations of the additive 0.95, 1.24 and 1.79% (wt%) were obtained. The length-wise and cross-sectional distributions of the nanoparticles in

the as-spun and the drawn nanocomposite filaments were investigated using burn-out tests, linear density and optical microscopy. Optical microscopy and scanning electron microscope (SEM) were used for analysing the dispersion and distribution of nanoparticles. UV and TGA were used for studying UVA protection and thermal stability of the extruded nanocomposites.

Materials

A fibre extrusion grade of isotactic polypropylene, MFI (melt flow index) = 27.84 g/10 min (standard method BS 1133:2000), supplied by Basell Polyolefins in granular form was used as the polymer matrix.

A commercial sample of nanoparticles metal oxide containing 98% titanium dioxide (TiO₂) and 2% manganese oxide (MnO) was obtained for compounding with the PP. This was received as a fine powder of particle size ranging from 60 nm to 200 nm, light brown colour, a melting point of 1830 °C, and bulk density of 290 kg/m³. The modification of TiO₂ with MnO is aimed at enhanced UVA (400–315 nm) absorption and reduced free radical generation, hence achieving better ageing properties.

Experimental technique and method

There are three common types of twin-screw extruders: (1) Intermeshing co-rotating twin screw, (2) Intermeshing counter-rotating twin screw, and (3) Non-intermeshing counter-rotating twin screw. Intermeshing twin-screw extruders have the following advantages in comparison to single-screw extruders (Chung 2000): (i) Positive conveying of polymer solid and melt along the screw channel, (ii) Better melting and mixing, (iii) Self-cleaning of the screw surface if fully intermeshing, (iv) Fast pressure buildup along the crew channel, and (v) short residence time distribution in each sequential zone, i.e. feeding and mixing. Non-intermeshing twin-screw extruder may be described as an intermediate of single-screw and intermeshing twin-screw extruders. They do not have self-cleaning capability, unlike intermeshing twin-screw extruders. They have better mixing and conveying capabilities than single-screw

extruders. They are often used for devolatilization of the solvents from concentrated polymer solutions.

Figure 1 shows the schematic diagram, profile and configuration of 10-mm twin-screw compounder/extruder made by (Rondol Technology Ltd., UK). The temperature profile of the twin screw has been divided into five heating zones: four of them (Z1, Z2, Z3, and Z4) for heating the twin screw, and the fifth one (Z5) for heating the die. In order to vent entrapped air, pressure release, moisture or volatile gases, there are two vents one before side feeder and the second between it and the die.

For high-shear mixing, an intermeshing corotating twin-screw profile was used (Fig. 1). The performance of an intermeshing corotating twin-screw extruder critically depends on the screw configuration. The desired screw configuration is obtained by assembling various screw elements on a screw shaft. The screw elements may be classified by their functions into two major categories: conveying/feed element (screw busing), and mixing element/block.

Conveying elements are used to convey polymer solids and melts along the screw. The polymer is positively transferred from one screw channel to the second screw channel in the intermeshing region by the wiping action of the intermeshing flight. The polymer makes ‘8-shape’ passing through both screws.

The mixing blocks with gear teeth is used to split the melt flow several times resulting in excellent distributive mixing. The gear teeth of these mixing elements on one screw do not have intermeshing corresponding gear on the other screw. Therefore, the mixing blocks provide well distributive mixing without high dispersive stresses (Chung 2000).

The polymer (PP) matrix was fed through the main feeder (hopper), whilst the nanoparticles (modified TiO₂) were introduced by the side feeder which was mainly designed for feeding nano and micro additives. The molten nanocomposite flow was quenched in water pass, and then the filaments were collected on a bobbin by winder. A set of nanocomposite filament samples with different TiO₂ concentrations (wt%) was obtained under the same extrusion conditions as given in Table 1. Three different concentrations of nano TiO₂ were purposed and encountered with the control sample 1 (neat PP). Burn-out test (ASTM D2584-02) has been used to find out the actual concentrations of the TiO₂ nanoparticles utilized in this study. Specimen lengths of 100 cm from the nanocomposite (PP + TiO₂) samples were tested to check the TiO₂ content and distribution within the extruded filaments. Each 100 cm length was cut into 4 × 25 cm and placed in four furnace boats with known weights and then heated to 600 °C

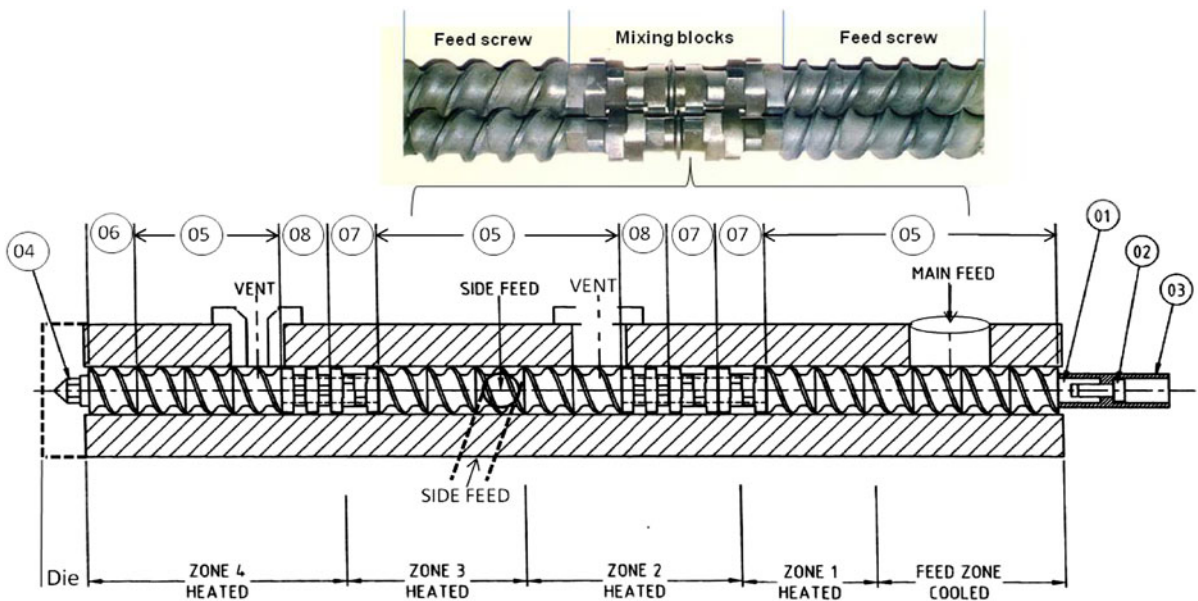


Fig. 1 Twin-screw extruder configuration and profile: 01 Hex Shaft, 02 Coupling retaining screw, 03 Coupling, 04 Screw tip, 05 Feed screw, 06 Extrusion screw, 07 Mixing block (4 × 60° Forw.), and 08 Mixing block (4 × 90° Alt.)

for 30 min. PP polymer will burn out, and TiO₂ will remain as a residual in the boat which will be weighed after 30 min cooling down, and finally the weight of TiO₂ will be determined and hence its percentage along the filament as given in Table 2. The consistency of TiO₂ content in the extruded nanocomposites indicates the good distribution of the nanoparticles along the tested samples 2 (0.95% TiO₂ in PP), 3 (1.24% TiO₂ in PP), and 4 (1.79% TiO₂ in PP).

As an alternative method to find the effect of nanoadditives in the extruded monofilaments, the linear density was determined. To find out the fibre count or Tex (yarn count), method of cutting and

weighing was used. Each yarn of 3.2 m was cut into 16 specimens of 0.2-m lengths, and each specimen was weighed individually using an accurate digital balance (up to four figures). The average weight of the 16 specimens was considered, and then Tex was calculated for the four samples.

The optical microscopy is used for investigating the extruded nanocomposites to evaluate the distribution of nano (TiO₂ and MnO) particles along and across filament axis. The average diameter of the produced monofilaments is ~500 μm and the modified TiO₂ is ranging from 60 to 200 nm in diameter.

In order to verify the improvement of thermal stability of the PP + TiO₂ nanocomposites, thermogravimetric analysis (TGA) test has been measured by using Mettler Toledo (TGA/DSC 1 Star System) at a heating rate of 10 °C/min from 25 to 600 °C under air flow of 50 mL/min.

Table 1 Extrusion conditions for producing nanocomposite (PP + TiO₂) filaments

Main feeder	2.87 g/min
Side feeder	1.8, 2.8, 4.0 scaling rate
Screw speed	181 rpm
Take-up speed	10 m/min
Screw dimension (L/D)	20:1
Die diameter	2 mm
Residence time in barrel	45 s
Zone 1	100 °C
Zone 2	190 °C
Zone 3	240 °C
Zone 4	235 °C
Zone 5 (die)	230 °C

Results and discussion

Figure 2 shows a linear trend of the measured linear density in Tex versus the content (wt%) of TiO₂ in the extruded filaments. The linear proportionality of the graph (Fig. 2) confirms the existence and increment of the nanoadditives in the nanocomposites produced.

Table 2 Results of burn-out test

Sample	Boat W _B (g)	B + fibre W _{BF} (g)	B + TiO ₂ W _{BT} (g)	Fibre W _F (g)	TiO ₂ W _T (g)	% Content of TiO ₂ = (W _T /W _F) × 100
2	7.1845	7.2557	7.1853	0.0712	0.0008	1.12
	6.2762	6.3433	6.2768	0.0671	0.0006	0.89
	6.7334	6.8118	6.7341	0.0784	0.0007	0.89
	12.6290	12.7078	12.6297	0.0788	0.0007	0.89
						0.95 ± 0.12
3	7.1853	7.2474	7.1861	0.0621	0.0008	1.29
	6.2768	6.3373	6.2775	0.0605	0.0007	1.16
	6.7340	6.7941	6.7347	0.0601	0.0007	1.16
	12.6296	12.6966	12.6305	0.0670	0.0009	1.34
						1.24 ± 0.09
4	7.1863	7.2643	7.1877	0.0780	0.0014	1.79
	6.2777	6.3436	6.2789	0.0659	0.0012	1.82
	6.7349	6.8022	6.7361	0.0673	0.0012	1.78
	12.6304	12.6988	12.6316	0.0684	0.0012	1.75
						1.79 ± 0.03

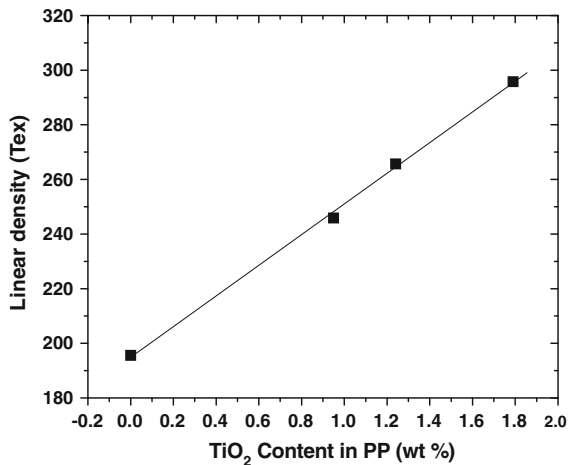
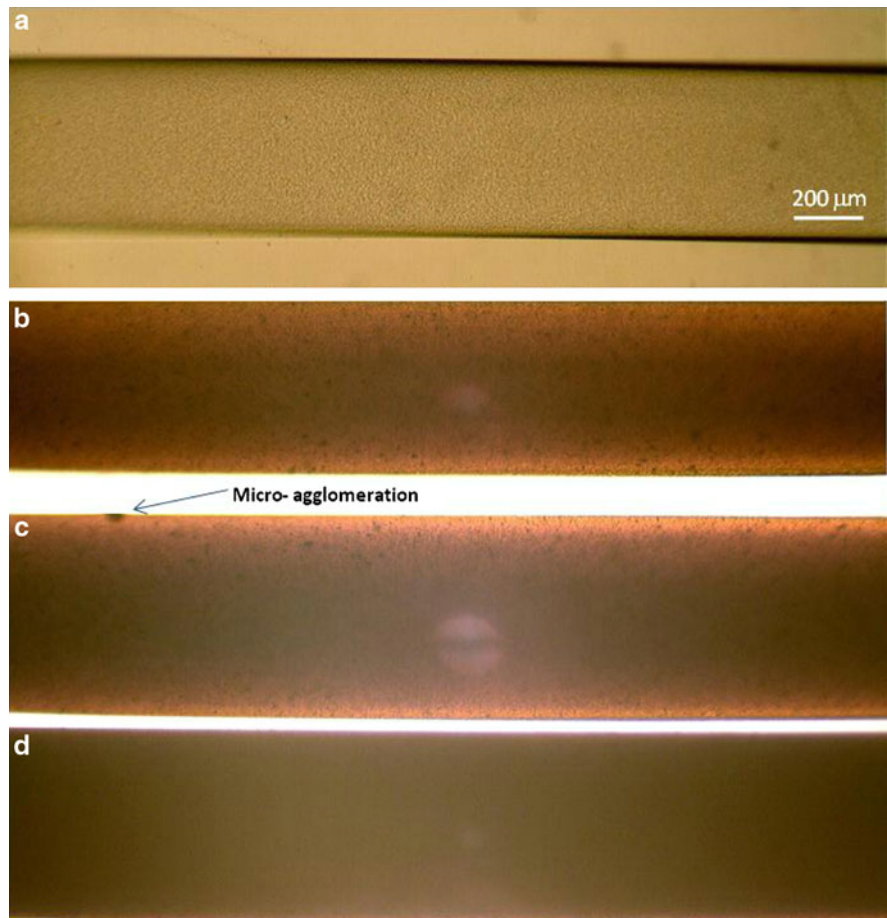


Fig. 2 Linear density versus the modified TiO₂ content (wt%) in nanocomposite (PP + TiO₂) filaments

Figure 3b–d shows a selection of the respective optical images of the as-spun nanocomposite (PP–TiO₂) filaments, when 0.95, 1.24 and 1.79% of

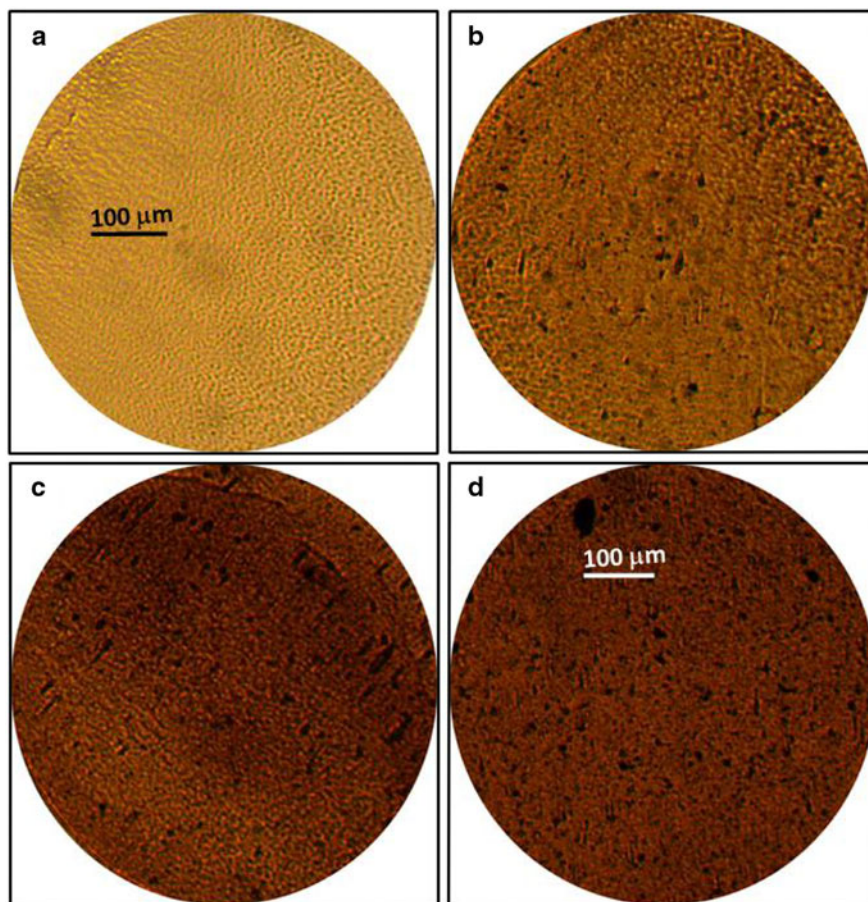
Fig. 3 Longitudinal sections of nanocomposite (PP + TiO₂) filament (as-spun) showing the distribution of nano TiO₂ along the filaments: (a) Neat PP, (b) 0.95% TiO₂ in PP, (c) 1.24% TiO₂ in PP and (d) 1.79% TiO₂ in PP



modified TiO₂ is added to the polypropylene. For comparison, a control sample (neat PP) is shown in Fig. 3a. In case of 0.95% metal oxide (TiO₂/MnO) in PP, the longitudinal sectional image (b) shows a good distribution of TiO₂ (black dots) along the filament as well as perfect dispersion of the manganese oxide (brownish colour). Although there are small clusters or micro agglomerated particles, there is a good distribution of the nano TiO₂ along the filament and well-dispersed MnO as shown in Fig. 3c. Figure 3d shows a longitudinal section of the nanocomposite doped with 1.79% of nanoparticles. Owing to the high increment of the modified TiO₂, the colour of the images (d) became darker than that shown in (b) and (c). This might be attributed also to good and uniform distribution of the nanoadditives along the nanocomposites produced.

Figure 4 presents another selection of the respective optical cross-sectional images of the as-spun nanocomposite (PP + TiO₂) filaments when 0.95,

Fig. 4 Cross sections of nanocomposite (PP + TiO₂) filament (as-spun) showing the distribution of nano TiO₂ across the filaments: (a) Neat PP, (b) 0.95% TiO₂ in PP, (c) 1.24% TiO₂ in PP and (d) 1.79% TiO₂ in PP

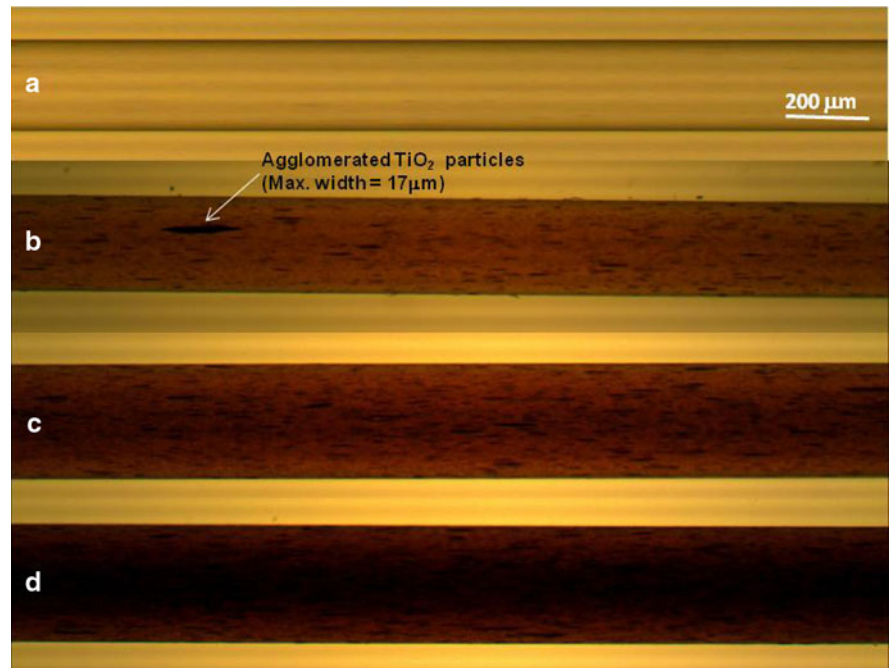


1.24 and 1.79% of modified TiO₂ is added to the polypropylene. Figure 4a also shows the cross section of the neat PP (control sample). Fig. 4b–d shows that there are few micro agglomerations in each section but the nanoadditives are well dispersed and distributed into the polymer matrix (PP). As seen clearly in Fig. 4d, in the largest agglomeration that we got in case of addition of 1.79% of metal oxide into the polymer, the size of this agglomerated particulate is $\sim 30 \mu\text{m} \times 50 \mu\text{m}$.

The nanocomposite samples have been cold drawn up to 13 times ($\text{DR} = 13$) under the same conditions. Figure 5b–d shows the respective optical images of longitudinal sections for the drawn nanocomposite (PP + TiO₂) filaments when 0.95, 1.24 and 1.79% of modified TiO₂ is added to the polypropylene. Figure 5a presents the drawn control sample (neat PP) which appears still the same, except that the thickness is reduced. Figure 5b shows the nanoparticle distribution along the drawn PP fibres doped

with 0.95% modified TiO₂. It is clear that the nanoadditives were present and distributed along the nanocomposite filaments as compared with the neat PP. As a comparison between the shapes of the agglomerated nanoparticles in both the as-spun and drawn filaments, it is obvious that the shape of the clusters in as-spun filaments seem to be round. However, in the case of the drawn filaments, they became elongated and were divided into short dashes and tiny spots. The height of the largest agglomeration in the drawn PP filament doped with 0.95% metal oxide is $17 \mu\text{m}$ as shown in Fig. 5b. Another optical image along the PP filaments filled with 1.24% metal oxide is shown in Fig. 5c, in which the count and existence of TiO₂ (black dashes and spots) and MnO (brownish colour) became significant as compared to Fig. 5a, b. The image is still showing good dispersion and distribution of the nanoadditives along the drawn nanocomposite (PP + TiO₂) fibres. In Fig. 5d as the content of the used nanoparticles increased to 1.79%,

Fig. 5 Longitudinal sections of nanocomposites (PP + TiO₂) filament (DR = 13) showing the distribution of nano TiO₂ along the filaments: (a) Neat PP, (b) 0.95% TiO₂ in PP, (c) 1.24% TiO₂ in PP and (d) 1.79% TiO₂ in PP



the filaments became darker and the agglomerations cannot be seen and evaluated properly, although the modified nano TiO₂ are well distributed.

In order to show the ability of using the side feeder of the twin screw for dispersing and distributed the nanoparticles into polymers, another trial has been done for blending the nanoparticles with polymer using an external blender. The polymer (PP) chips were granulated to fine powder and then transferred with the nanoparticles (TiO₂) to the external blender for mixing. The mixed powder was fed via the main feeder (hopper) of the twin screw under the same extrusion conditions (Table 1), when some PP filaments doped with 1.95% modified TiO₂ were produced. Figure 6 shows a selection of the optical images of the nanocomposites extruded by the external blender along the filament. On comparison with Fig. 3, it is clear that the rate of clusters/agglomerations (black particulates) shown in Fig. 6 is significant. This is to confirm that good mixing, dispersion and distribution of nanoparticles into polymers can be achieved by using the side feeding technology of the 10 mm twin-screw extruder.

SEM was also used to image and characterize the dispersion of TiO₂ nanoparticles and their distribution in the nanocomposites. Figure 7 shows SEM

images of four samples: (a) neat PP, (b) PP + 0.95%TiO₂, (c) PP + 1.24%TiO₂, and (d) PP + 1.79%TiO₂. It is clear that the TiO₂ particles are well distributed on the surfaces of the nanocomposites, and there are small clusters in which the size of the agglomerated particles is ranging between 80 and 443 nm (Fig. 7). These SEM images and above optical scans confirmed the dispersion of TiO₂ into PP matrix and showed that they are well distributed along and across (PP + TiO₂) nanocomposites.

Further to the above qualitative analysis of dispersing and distributing the nanoparticles into the polymer, a quantitative analysis of the extruded nanocomposites was carried out to evaluate the influence of adding TiO₂ to PP. UV and TGA analysis have been used to test the functionality of the nanocomposites based on the effect of imparting metal oxide to the polymer matrix.

Using UV spectrophotometer, the neat PP and PP + TiO₂ nanocomposites are exposed to a beam of wavelengths ranging from 300 nm to 450 nm; this is to cover UVA range. Figure 8 displays the UV–Vis spectra for the as-spun samples, in which the % absorbance is converted to % transmittance; this is to make it easier for comparing the samples of different TiO₂ contents. As expected, the neat PP (curve 1) transmits all the wavelengths and does not

Fig. 6 Longitudinal sections of nanocomposites (PP + TiO₂) filament (as-spun) showing the distribution of 1.95% of nanoparticles (TiO₂) along the filament produced via an external blender not the side feeder

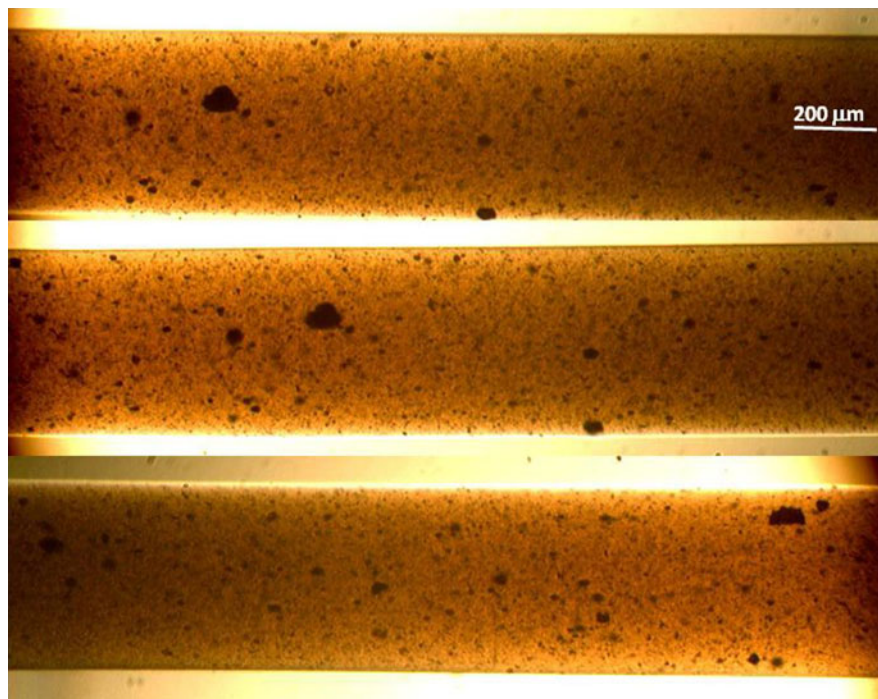
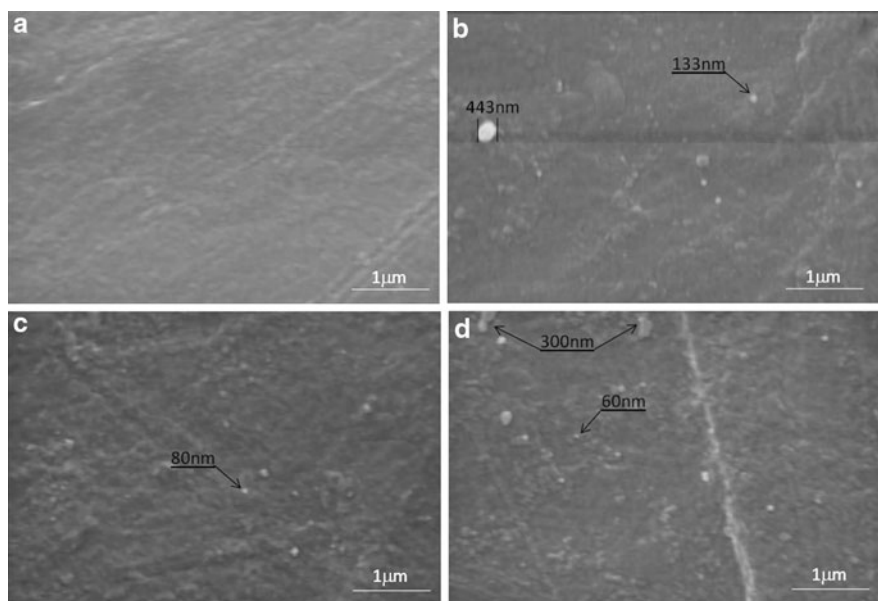


Fig. 7 SEM images of as-spun nanocomposites: (a) Neat PP, (b) PP + 0.95% TiO₂, (c) PP + 1.24% TiO₂ and (d) PP + 1.79% TiO₂



absorb or block any UV. However, in case of existence TiO₂, it is clear that the nanocomposite (PP + 0.95% TiO₂), curve 2, transmits and damps the wavelengths up to 349 nm, and thereafter the UV has been totally absorbed. By increasing TiO₂ content, the UV absorbance increases and transmittance decreases as has been shown in case of

PP + 1.24% TiO₂ (curve 3) and PP + 1.79% TiO₂ (curve 4). For more details and confirming the significant improvement of UV protection for the nanocomposites, Table 3 gives the values of the corresponding wavelengths at which the UV was totally absorbed, and stopped from going through the nanocomposites.

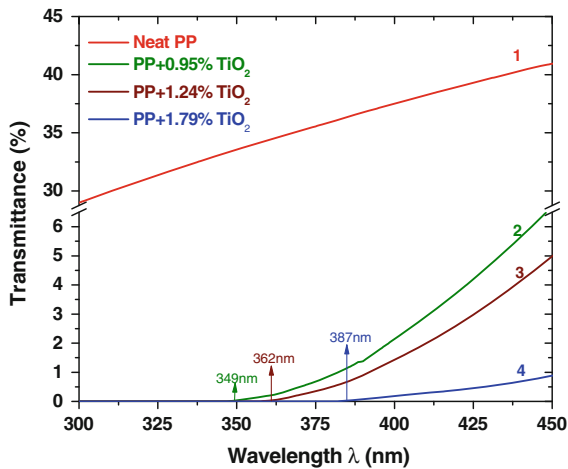


Fig. 8 UV–Vis spectra for neat PP and nanocomposites (PP + TiO₂)

Table 3 Wavelengths of UV-absorption for the extruded nanocomposites

Sample	UV absorbed wavelength (nm)
Neat PP	NA
PP + 0.95% metal oxide	349
PP + 1.24% metal oxide	362
PP + 1.79% metal oxide	387

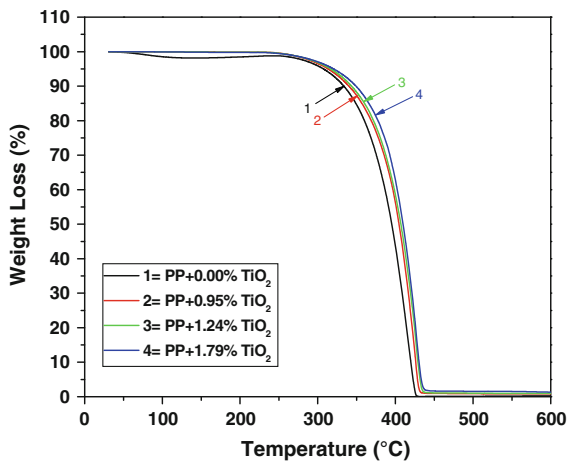


Fig. 9 TGA for neat PP and nanocomposites (PP + TiO₂)

Figure 9 shows the TGA graphs of the as-spun nanocomposites compared with the neat PP, in which the % weight loss versus the temperature are displayed as curves 1, 2, 3 and 4 corresponding to

Table 4 TGA decomposition temperatures of (PP + metal oxide) nanocomposites

Sample	Temperature (°C) at different % weight loss			
	95 wt%	75 wt%	50 wt%	25 wt%
PP + 0.00% metal oxide	307.34	368.59	395.34	411.52
PP + 0.95% metal oxide	313.28	377.77	404.48	419.24
PP + 1.24% metal oxide	316.44	380.34	406.86	421.97
PP + 1.79% metal oxide	320.16	385.74	409.81	423.93

Table 5 % Content of nano TiO₂ and % weight loss of the nanocomposites at 500 °C

Sample	Burn out test % content of TiO ₂ in nanocomposites at 600 °C	TGA test % weight loss at 500 °C
2	0.95	0.89
3	1.24	1.04
4	1.79	1.57

the four samples. From this figure and Table 4, the properties of thermal decomposition of the nanocomposite fibres were analysed, and it is found that the higher percentage of nano-metal oxide the higher thermal stability nanocomposites. This is because by imparting nano TiO₂ and MnO particles to PP, the nanocomposite becomes more thermally stabilized and TGA decomposition rate becomes much slower than that of the neat PP (see Table 4). Table 5 gives the summary of burn-out test concerning the actual concentration of nano TiO₂ in the extruded nanocomposites compared with the TGA % weight loss at 500 °C. It is clear that the TGA weight loss residue is corroborated to the nanoparticle concentrations used with slightly difference between the values, which might be because of the difference in temperatures (600 and 500 °C) and amount of tested specimens.

Conclusion

A 10-mm twin screw has been used in this study to achieve good compounding of a nano-powder and polymer. By feeding polymer granules and nanoparticles at the same time via main and side feeders of the twin screw, nanocomposite filaments doped with well-dispersed and distributed nanoparticles were obtained.

A comparison of the nanoparticles distribution obtained via the side feeder, with that processed by the external blender. based on the results of optical microscopy and SEM, showed that a good distribution was observed using the side feeding technology. UV and TGA analysis present promising results confirming that the presence of the modified TiO₂ nanoparticles significantly improved UV absorption and thermal stability of polypropylene fibres.

Acknowledgements The authors acknowledge with thanks for the appreciable help by and useful discussion with Prof. A. A. Hamza (President of the British University in Egypt) and Dr. M. R. Mahmoudi (School of Design, University of Leeds, UK). The authors further thank FET Ltd. UK for offering them with a commercial sample of nanometal oxide.

References

- Alexandre M, Dubois PH (2000) Polymer-layered silicate nanocomposite preparation, properties and uses of new class materials. *Mater Sci Eng* 28:1–63
- Ash BJ, Schadler RWS, Apple T, Benicewicz BC, Roger DF, Wiegand CJ (2002) Mechanical properties of Al₂O₃/polymethylmethacrylate nanocomposites. *Polym Compos* 23:1014–1025
- Chiu CW, Lin CA, Hong PD (2010) Melt-spinning and thermal stability behavior of TiO₂ nanoparticle/polypropylene nanocomposite fibers. *J Polym Res*. doi:10.1007/s10965-010-9426-0
- Chung CI (2000) *Extrusion of polymers theory and practice*, Ch. 1. Hanser, Munich
- El-Dessouky HM, Mahmoudi MR, Lawrence CA, Yassien KM, Sokkar TZN, Hamza AA (2009) On the physical behavior of isotactic polypropylene fibers extruded at different draw-down ratios. I. Optical properties and cold-drawing. *Polym Eng Sci* 49:2116–2124
- Erdem N, Erdogan UH, Cireli AA, Onar N (2010) Structural and ultraviolet-protective properties of nano-TiO₂-doped polypropylene filaments. *J Appl Polym Sci* 115:152–157
- Jose J, Abdul KM (1999) Impedance spectroscopic analysis of AC response of nanophase ZnO and ZnO-Al₂O₃ nanocomposites. *Nanostructured Mater* 11:1091–1099
- Kumar AP, Depan D, Tomer NS, Singh RP (2009) Nanoscale particles for polymer degradation and stabilization—trends and future perspectives. *Prog Polym Sci* 34:479–515
- Pane S, Tedesco R, Greger R (2001) Acrylic fabrics treated with plasma for outdoor applications. *J Ind Text* 31:135–145
- Ray SS, Okamoto M (2003) Polymer/layered silicate nanocomposites: a review from preparation to processing. *Prog Polym Sci* 28:1539–1641
- Sawhney APS, Condon B, Singh KV, Pang SS, Li G, Hui D (2008) Modern applications of nanotechnology in textiles. *Text Res J* 78:731–739
- Schmidt G, Malwitz MM (2003) Properties of polymer–nanoparticle composites. *Curr Opin Colloid Interface Sci* 8:103–108
- Wang Z, Li HL (2002) Highly ordered zinc oxide nanotubules synthesized within the anodic aluminium oxide template. *Appl Phys A* 74:201–203
- Wei Q, Yu L, Mather RR, Wang X (2007) Preparation and characterization of titanium dioxide nanocomposite fibres. *J Mater Sci* 42:8001–8005
- Wong YWH, Yuen CWM, Leung MYS, Ku SKA, Lam HLI (2006) Selected applications of nanotechnology in textiles. *AUTEX Res J* 6:1–8
- Yeo SY, Lee HJ, Jeong SH (2003) Preparation of nanocomposite fibers for permanent antibacterial effect. *J Mater Sci* 38:2143–2147